APPLICATION OF BEAM-FORMING USING DECONVOLUTION METHOD TO THE DEVELOPMENT OF THE NEW LAUNCH PAD OF EPSILON

Yutaka Ishii[1], Tatsuya Ishii[3], Jørgen Hald[2], Hideshi Oinuma[3], Seiji Tsutumi[3] and Kyoichi Ui[3]

[1] Brüel & Kjaer Japan
2-6 Kanda-Tsukasamachi, Chiyoda-ku, Tokyo 101-0048, Japan
[2] Brüel & Kjaer SVM A/S, Denmark
[3] Japan Aerospace Exploration Agency (JAXA), Japan

ABSTRACT

In 2013, the Japan Aerospace Exploration Agency (JAXA) launched Epsilon, a new launch vehicle. A new launch pad was designed for decreasing the sound pressure levels during lift-off. A sub-scale launch pad model was experimentally investigated before determining the final design. A commercially available Beamforming system, composed of a foldable array structure and including a deconvolution calculation algorithm, was applied to the sub-scale model tests to clarify the contribution to the sound pressure at the payload, focusing on the jet plume spread behind the launch pad model. This paper describes a beamforming system and the results of application to sub-scale model tests of the rocket launch pad. In addition, the paper presents the sound data measured with hydrophones in far-field at the time of the first launch of the Epsilon in 2013.

1   INTRODUCTION

1.1   Beamforming System as a Tool

Beamforming is a well-established technique for sound source localization. Over the last two decades, many commercial beamforming systems have become available, the systems being based on various types of array design [1, 2, 3]. When we consider applying a beamforming system to measure at long distances, it is usually necessary to apply an array with large diameter to achieve acceptable spatial resolution [4, 5]. Typically, Diagonal Removal will be used to minimize the effect of flow noise in the individual microphones, and deconvolution can be used to suppress sidelobes and enhance resolution [4, 5, 6, 7]. Moreover, it is necessary that a mechanical design of the array supports easy, quick and precise deployment at a site. We applied the beamforming system to outdoor tests of the launch pad of a scale-model rocket. Since the frequencies of interest become higher in scale model tests than in full-scale tests, where very

low frequencies are dominating, an adequate resolution can be achieved with an array of manageable size. Beamforming provides an angular resolution of the contributions to the sound pressure measured at the array. In connection with rocket launch, the sound radiated towards the payload at the top of the rocket is of primary interest. The array should therefore be positioned in or close to the direction from the launch pad to the top of the rocket.

1.2   Application of Beamforming to R&D of Epsilon Launch Vehicle

The motivation of this paper comes from the problems related to the launch vehicle acoustics. The rocket motor emits high-speed jet plume during its lift-off. This high-speed jet in general forms intensive sound sources through its shock-associated waves and its impingement on ground structures like launch pad. The launch vehicle when exposed to the intensive acoustic environment sometimes suffers from malfunctions of the payloads.

JAXA's new solid propellant launch vehicle, named Epsilon, planned its first launch in 2013. The Epsilon launch vehicle, composed of three-stage motors, has a potential of putting 1.2 t payload to low-earth-orbit (LEO). The specifications of Epsilon is available in reference [8, 9, 10]. The Epsilon takes over the existing launch site, Uchinoura Space Center (USC). Figure. 1 compares the launch pads used for the former M-V launch vehicle and the present Epsilon. It is anticipated that intensive sound waves are fed-back from the deflected jet plume. Thus, the project team aimed at mitigating the acoustic environment around the vehicle without massive facilities such as water injection and long flue.

Two types of research activities, computational and experimental, have progressed in order to understand the mechanism of sound generation and validate the acoustic environment around vehicle. These activities suggested the launch pad to alleviate the sound generation by changing the deflection angle, covering the deflected plume, and scattering Mach waves [11, 12].

This paper focuses on the final subscale-model tests to finalize the new launch pad design to lessen the acoustic impact on the vehicle. The measurement and results by the beamforming system applied to the subscale-model tests are described below. In addition, this paper briefly mentions the measurement results obtained by hydrophones at the first launch of Epsilon.

Fig. 1. USC Launch Pad. Before Refurbishment for M-V Vehicle (left) and Present Structure for Epsilon (middle and right).

2   BEAMFORMING SYSTEM

2.1   Array geometry and Theory

Array geometry is one of the key factors to obtain good results from a beamforming system. A good array geometry is characterized by having low Maximum Sidelobe Level (MSL). The MSL can be defined as the relative difference in dB between the main lobe and the highest side lobe of beamformer. Many types of optimized irregular arrays for beamforming such as Full Wheel Arrays, Half Wheel Arrays, Sliced Wheel Arrays and Multi-armed Foldable Arrays have been introduced and are commercially available.

As illustrated in Fig. 2 (a), we consider a planar array of *M* microphones at M distributed locations $\mathbf{r}_m$ (m=1, 2,….,M) in the *xy*-plane of our coordinate system [6, 7]. When such an array is applied for Delay And Sum (DAS) Beamforming, the measured pressure signals p_m are individually delayed and then summed:

$$b(\boldsymbol{\kappa},t) = \sum_{m=1}^{M} p_m(t - \Delta_m(\boldsymbol{\kappa}))$$ (1)

Here, $\boldsymbol{\kappa}$ is a unit vector in the focus direction.

The frequency domain version of Eq. (1) for the DAS beamformer output is:

$$B(\boldsymbol{\kappa},\omega) = \sum_{m=1}^{M} P_m(\omega)e^{-j\omega\Delta_m(\boldsymbol{\kappa})} = \sum_{m=1}^{M} P_m(\omega)e^{j\mathbf{k}\cdot\mathbf{r}_m}.$$ (2)

In this equation, $\mathbf{k} \equiv -k\boldsymbol{\kappa}$ is the wavenumber vector of a plane wave incident from the direction $\boldsymbol{\kappa}$.

The frequency domain beamformer will have a "main lobe" of high directional sensitivity around the focus directions, although with some lower "side lobes" as shown in Fig. 2 (b). The spatial resolution, R, of DAS beamforming is approximately

$$R = 1.22\lambda \frac{L}{D}$$ (3)

where *L* is the measurement distance, *D* is the array diameter, and λ is wavelength [2]. The measurement distance, *L*, should not be much smaller than the array diameter, *D*. Also from Eq. (3), the spatial resolution, *R*, is inversely proportional to the array diameter, *D*. So if the wavelength and/or measurement distance is large (low frequencies), then a large array diameter is needed to retain a certain resolution.
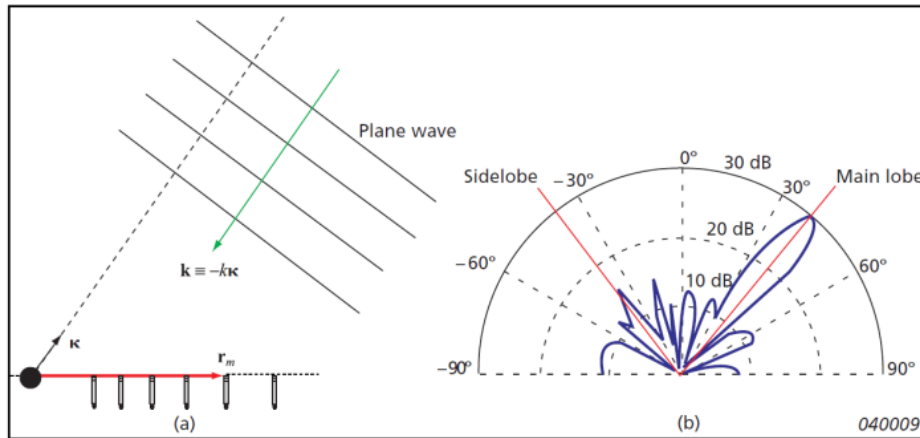
Fig. 2. (a): Microphone array, a far-field focus direction, and a plane wave incident from the focus direction. (b): Directional sensitivity diagram with main lobe in the focus direction and lower side lobes in other directions.

2.2   Beamforming with deconvolution calculation

Using iterative deconvolution techniques, it is possible to achieve a higher resolution than that provided by standard DAS beamforming techniques [4, 13]. The idea is that when measuring on a point source, the DAS beamforming pressure power result is given by the location of the point source convolved by the beamformer's directional characteristics as shown in Fig. 2(b) and produces what is known as the point-spread function, PSF. For a given beamformer array design, this PSF is known and can be compensated for using deconvolution techniques. This deconvolution gives a possibility to increase the spatial resolution of acoustic arrays and reduce disturbing side lobe effects. In many fields of imaging, for example optical and radio astronomy, deconvolution methods are widely used to increase the spatial resolution. For that purpose, a variety of algorithms have been developed in the past, for example the Non Negative Least Squares (NNLS) algorithm [4, 13]. In the PULSE Beamforming software, FFT-NNLS can be used in the calculation.

2.3   Shading function

In the practical outdoor measurement, shading function [4, 6, 7] is useful to avoid the effect of coherence loss induced by turbulence. A main effect of air turbulence is a distortion of the wave fronts arriving at the array as shown in Fig. 3.
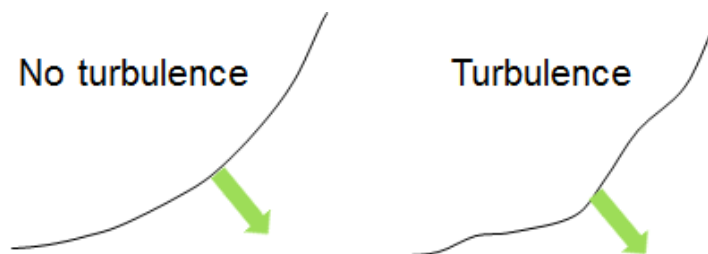

Fig. 3. Sound wave front without (left) and with (right) turbulence.

This distortion has the effect of adding phase modulation to the microphone signals. Especially, for wider microphone separation like in a large array, the modulation will become

more incoherent and that reduces coherence between the measured microphone signals. When shading is applied, effectively only a frequency-dependent central subset of the microphones will be used in the DAS beamforming calculation. With no turbulence, the full array can be used (no shading). With more turbulence and at higher frequencies, a smaller central part of the array will be used as shown in Fig. 4.
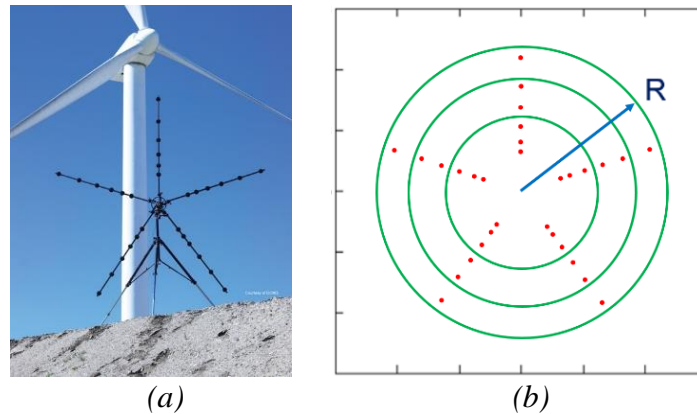

(a)   *(b)*

Fig. 4. (a): Array example with five arms and 30 microphones. (b): Area used for none, some and much turbulence.

2.4   System Overview

The beamforming system consists of an optimized irregular array, a front-end system and data acquisition software including beamforming calculation which can apply deconvolution calculation and shading function. Typically, 3.5 m diameter five-arm foldable array or 2.5 meter diameter 9-arm foldable array that can be quickly deployed at the measurement site may be useful for outdoor measurements.

2.5   Example: Jet Engine Measurement

A compact beamforming system has been applied to the jet engine ground tests. Brüel & Kjaer Japan together with JAXA has carried out source localization in the ground static operation of a turbojet engine in open test site [14]. The primary role of the source localization was to map the jet noise source behind the nozzle of the demonstration engine. Figure. 5(a) shows the five-arm foldable microphone array and a small turbojet engine. The microphone array is located behind the engine so that the array focuses on the jet axis downstream of the nozzle.

The contours in Fig. 5(b) indicate the source distribution behind the nozzle, comparing a baseline conical nozzle (top) with a nozzle with mixing nails (bottom). The noise at middle frequency, i.e., 800 Hz in 1/3 octave band, corresponds to the broadband peak frequency of the jet noise of this engine at 85% engine rating (see the left column of the figure). It is clearly found that the source level far downstream of the nozzle is suppressed. This is because of the enhanced mixing by the mechanical mixer. Contrarily, the contour plots at higher frequencies, here the 3150 Hz band, suggests an increase in the source level due to the mixer. These results agreed well with the far-field sound pressure levels at side directions of the engine: those data were obtained simultaneously during the engine operation.

The applied five-arm foldable array is a simple system composed of quite few microphones. However, it is a useful tool to judge whether the designed structures or proposed concepts are promising from the acoustic point of view. Thus, the authors decided to use the results from a similar beamforming system in the subscale model tests of a new solid rocket motor for the Epsilon launch vehicle.
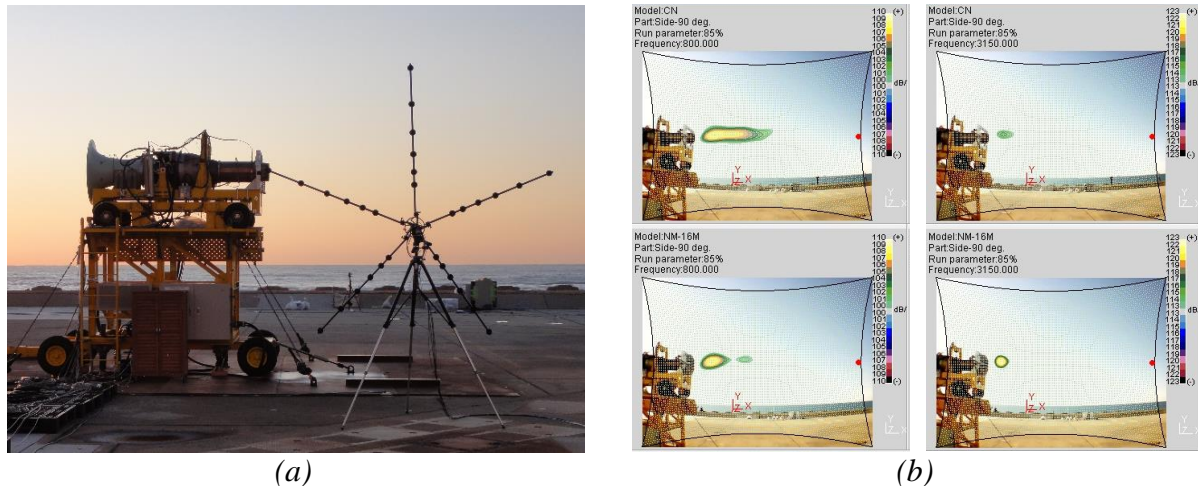

(a)　　　　　　　　　　　　　　　　　　　*(b)*

Fig. 5. (a): Five-arm foldable microphone array applied to engine test. (b): Example of measurement using a turbojet engine. SPLs of baseline nozzle at 85% engine rating (top), and with mixer nozzle (bottom).

3   APPLICATION TO SUBSCALE ROCKET MOTOR

3.1   Subscale-model Measurement for Acoustic Prediction (SMAP)

It was necessary to preliminarily estimate the acoustic influence of the solid rocket motor on the launch vehicle during lift-off. Primary acoustic concern was the design of the ground structure of the launch pad including the geometry of the tunnel that connects to the exhaust of the rocket motor. Acoustic prediction by empirical and computational fluid dynamic approaches supported the design of the launch pad structure. A subscale-model test campaign, called SMAP, was started to validate the computational prediction and finalize the design of the launch pad [11, 12].

Subscale solid rocket motor, as shown in Fig. 6(a), was used throughout the SMAP series. The ingredient of the solid propellant is similar to that of SRB-A, the first stage motor of the Epsilon. The 1/42 scale nozzle has a diameter of 41 mm. The expected Mach number is 3.3, and the corresponding Reynolds number is of the order of 105. Estimated thrust is about 1 kN, and the burning continues about 2 s.

The first and second series of SMAP contributed to validating the computational results and pointing out the effect of fence over the deflector. The last series, SMAP-3, and then focused on finalizing the launch pad geometry that would cause the minimum acoustic impact on the vehicle. In addition to the conventional measurement configuration, the microphone array system was employed as a reference.

(a)   (b)

Fig. 6. (a): Subscale Rocket Motor and Launch Pad Model on Flat Plate. (b): Gate-Type Test Stand for SMAP-3 Including Microphone Array.

3.2   Experimental Setup for SMAP-3

The subscale rocket motor was vertically settled at the end of the strut hanging on the middle of the gate-type test stand (see Fig. 6(b)). Beneath the motor was a launch pad model, i.e., a deflector, on the flat and rigid surface. The vertically introduced jet plume is deflected to the horizontal direction. The emitted jet spreads over the flat surface.

Three types of deflectors were proposed and experimentally investigated on their acoustic outputs as illustrated in Fig. 7. One is the baseline without extended duct (flue). The deflected high-speed plume is exposed to atmosphere and thus intensive sound sources are in the direct sight of vehicle. Other two deflectors have a flue after the plume deflection. One has a gradually changing cross-sectional geometry toward the high-aspect-ratio rectangular exit. The other maintains the cross-sectional geometry to the end.

Quarter-inch microphones were located in the far field of the deflector and around the motor casing (near field). All time signals were recorded and stored into hard disc at sampling rate of 200 kHz [15].
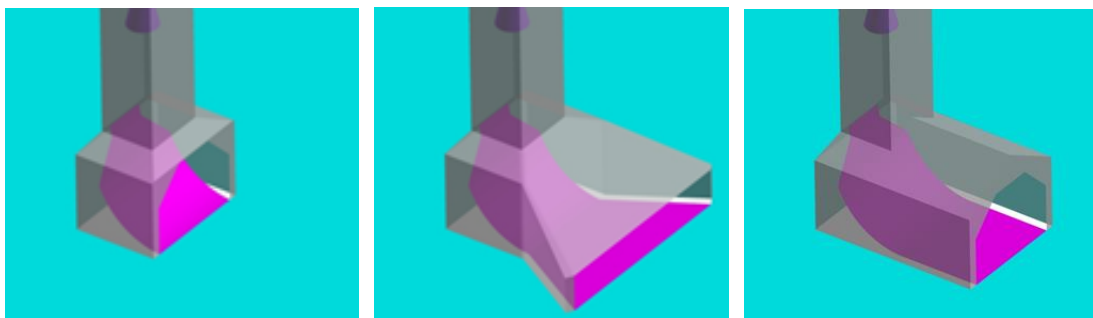

Fig. 7. Tested Deflectors: Baseline (left), Type-1 with High-Aspect-ratio Exit (middle), and Type-2 with Straight Flue (right).

3.3 Phased Array Measurement Setup, Test Conditions and Data Analysis

The array employed in the test campaign was a 2.5 m diameter 9-arm foldable array. Figure. 8(a) and 8(b) show the setup of the array. Each of the arms of the array had 6 microphones and all microphones were fitted with windscreens and covered with fire resistant cloths. The target area was smaller than the target area of the jet engine measurement in section 2.5 since the primary concern of the sound source was the jet plume on the ground surface. However, it was difficult to place the array closer to the object because of the existence of other structure and avoiding the fire of the rocket. The array was suspended from the top structure of the test stand. The focus point of the array was the tunnel exit of the sub-scale model of the launch pad and the distance from the array was 4.2 meter. The array covered angles from 35° to 65° relative to the ground. The array can also take a funnel shaped configuration, but the fully unfolded configuration was chosen since the space behind the array was the sky. Figure. 9 shows the MSL of the 2.5 m diameter 9-arm foldable array with 54 microphones in the fully unfolded configuration. It can be seen that the MSL is better than 7 dB to beyond 12 kHz. The ratio of the scale model was 1/42. Consequently, 12 kHz corresponds to 279 Hz for the full-scale model.
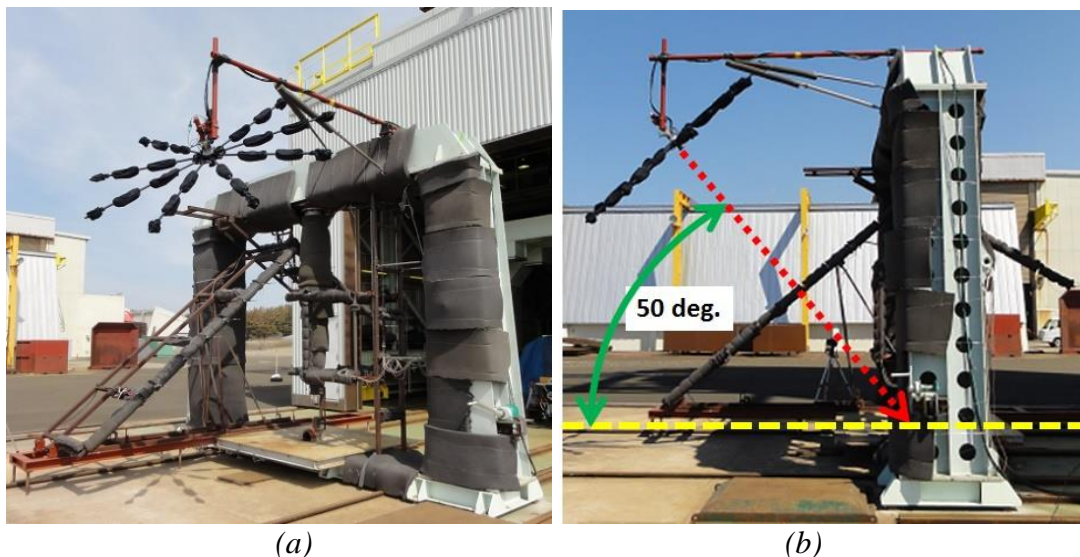

(a)   (b)

Fig. 8. (a): The array was suspended from the top structure of the test stand. (b): The array was focused on the exit of the deflector.
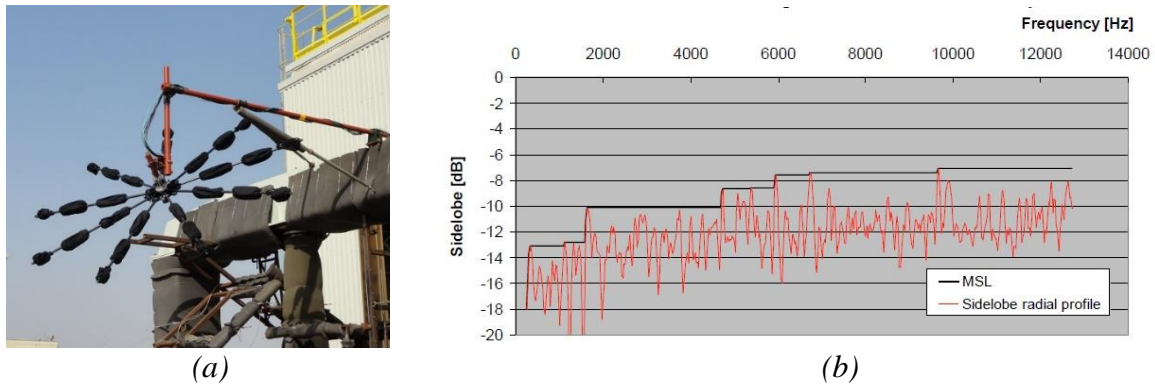
Fig. 9. (a): 9-arm foldable array applied to the tests. (b) MSL of the 2.5 m diameter 9-arm foldable array with 56 microphones in the fully unfolded configuration.

The sound was recorded for 20 s at 65.536 kHz sampling rate using Brüel & Kjaer PULSE system. An example of the measured signal is shown in Fig. 10. FFT was applied only on the shaded time interval, and the number of FFT lines was 6400. Shading and diagonal removal were also used in the beamforming calculation.
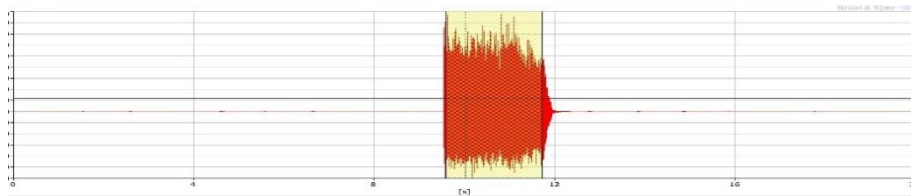

Fig. 10. Example of the measured signal. The shaded time interval was used for the calculation.

During the calculations, frequency bands were synthesized as shown in the Table 1.

Table 1. Synthesized frequency bands and corresponding octave band for the full-scale model

Synthesized frequency bands for the scale model	Corresponding octave band for the full-scale model
1876 Hz – 3744 Hz	63 Hz
3744 Hz – 7476 Hz	125 Hz
7476 Hz – 14912 Hz	250 Hz

4   RESULTS AND DISCUSSION

4.1   Sound Source Identification

Beamforming calculation was applied to the measured data to investigate the level and origin of the sound radiated upward from the launch pad models. As mentioned earlier, FFT-NNLS, diagonal removal and shading were used in the beamforming calculation. The results of the launch pad models, Type-1 (shown in Fig. 11 (left)) and Type-2 (shown in Fig. 11 (right)) were compared in three frequency bands corresponding to the 63 Hz, 125 Hz and 250 Hz octave band for the full-scale model. The range of the maps is 15 dB and the maximum scale of the maps for each frequency band are aligned.

Fig. 11. Launch Pad Model: Type-1 (left), and Type-2 (right)

In all three frequency bands, the result maps of Type-1 depict that the jet plume spread widely with higher level at the exit of the deflector compared with the result maps of Type-2 (see Fig. 12). To clarify the pressure contribution at the array centre, the pressure contribution density in the maps were integrated over the small selected area around the exit of deflectors. The size of the selected areas both on Type-1 and Type-2 are the same as shown in Fig. 13, and the pressure contribution at the array centre from them are shown in Fig. 14.
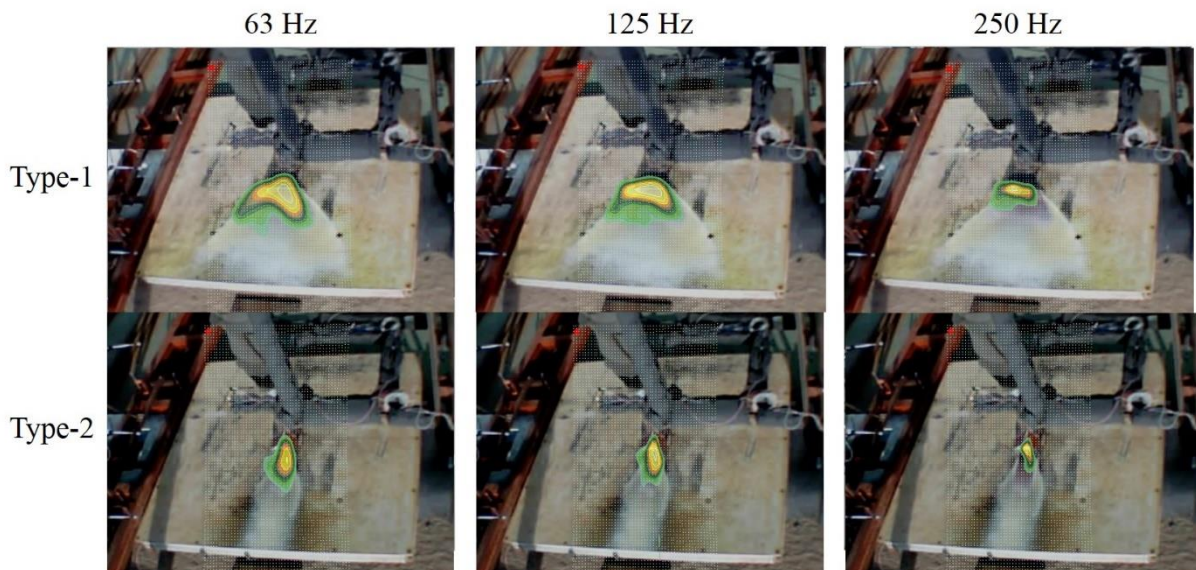

Fig. 12. Pressure Contribution Density maps for corresponding Octave bands for the full-scale model. The display range is 15 dB.
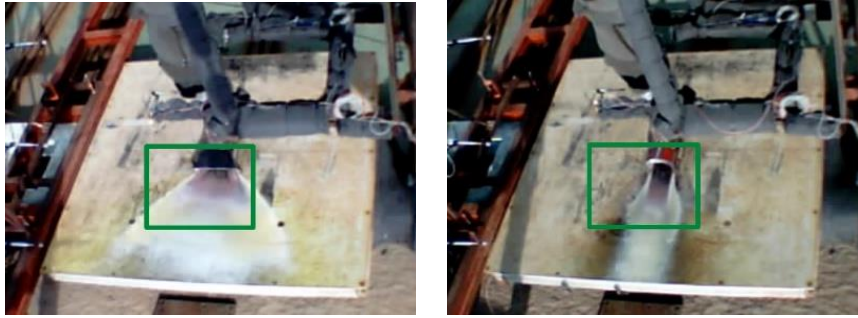
Fig. 13. Selected area for the area integration on Type-1 (left), and Type-2 (right).
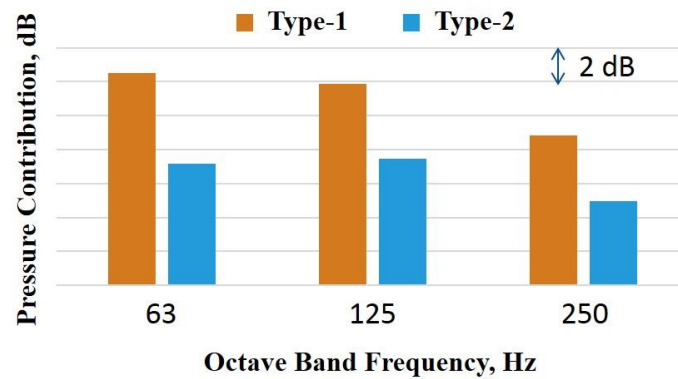

Fig. 14. Pressure Contribution at the Array Centre for Octave bands

The sound radiated towards the top of the subscale rocket motor could not be covered by the array measurements for the reason mentioned earlier. However, the results from both the maps and the pressure contribution at the array centre indicate the launch pad scale model Type-2 reduced the sound radiating upward.

4.2 Sound Pressure Levels in the Far Field

Sound pressure levels in the far field of the deflector exit are compared in Fig. 15. Considering the angular position of the phased array, the spectra in the figure are obtained at 50° from ground level. Octave band frequency is corrected based on the scale factor of the model. As is deduced from the abovementioned results by the beamforming, the deflector Type-2 provides reduced SPL in 63 Hz band compared with Type-1 (see Fig. 15). The far-field SPL is a sum of SPL's from all sound sources including that at the exit of the deflector. It is noted that the difference in SPL in other frequency band may be affected by sound sources other than the jet plume emitted from the deflector. The beamforming system suggested that the Type-2 deflector introduces weaker sound sources than the Type-1 deflector (see Fig. 12).
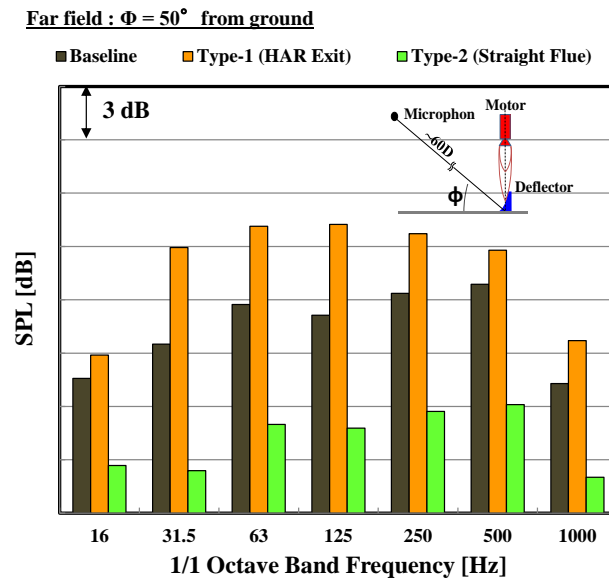
11

Far field : Φ = 50° from ground

■ Baseline   ■ Type-1 (HAR Exit)   ■ Type-2 (Straight Flue)

Fig. 15. Comparison of the SPLs obtained by the tested deflectors. The far-field SPLs at 50° above the ground level: similar direction toward the microphone array.

4.3   Setup for Sound Measurement

When we think about applying a beamforming system to investigate sound source location during the full-scale rocket launch, the use of a bigger array would be required, because the measurement distance would become long and frequencies of emitted sound would also become low. Moreover, we need to consider about the acoustic transducers to be employed in the array because the measurement would be carried out under extreme environmental conditions that could damage ordinary microphones or affect their performance, by being exposed to such factors as high sound pressure, rain or water. The use of hydrophones is one of the solutions that allows the use of acoustic transducers in such an environment. Typically, hydrophones are used in water, but they can be used in air as well. To investigate the possibility of using hydrophones in the measurements of the rocket launch, two hydrophones (Brüel and Kjær Type 8103) were employed at the first launch of Epsilon. One was put on a flat steel plate placed on the ground, and the other was placed on the top of a stand with 1 m height.

4.4   Example of Acoustic Data at the First Launch of Epsilon

Time date are shown in Fig. 16 [16]. Measurement at other positions than the hydrophone was done by traditional 1-inch piezo-electric microphone, Endevco Type 2510. Among them, a combination of the piezo microphone with a circular cowl, called "dish", was placed on the ground surface far away from the deflector (see Fig. 16). At the center of the 1800 mm-diameter of "dish", the microphone was flush-mounted with a water-proof grid.

The available data length was less than a few seconds because the vehicle climbs up quickly and acoustic properties varies. Another reason of the limited time signals is damage of the sensors and communication cables due to the exposure of high-temperature gas. Steep increase in pressure amplitude occurred after ignition, then high levels of amplitude were kept for a few seconds, and then the amplitude extremely increased (not shown in the figure), which indicates damages of sensors.

In the figure, it is found that the hydrophone gave similar time data with traditional sensor outputs. Results of frequency analysis are compared in Fig. 17 in the form of octave band levels. All spectra are not corrected for ground reflection and distance attenuation. Time duration for the analysis was chosen between $0.5 - 2.0$ s, as indicated in the top left graph of Fig. 16. During that time span, the height of the nozzle is expected to remain within six times the nozzle exit diameter [17]. This fact implies that there exists small gap between the nozzle and the inlet of deflector, and thus the dominant sound source is at the exit of the deflector. The spectrum at the deflector exit, thus, represents the sound source characteristics, having broad band peak in 250 and 500 Hz bands. As the microphone at the launcher top represents the acoustic environment outside the fairing, acoustic characteristics to be controlled are referred to this point. The spectral shape of the signal measured on the "dish" agreed well with the launcher top result. Considering the direct path to both the launcher top and surface ground from the jet plume, it is reasonable that the similar spectra are obtained at both points when directivity is small. The data obtained by hydrophones appear to coincide with the sound source spectra although they include the effects of reflection and propagation loss.
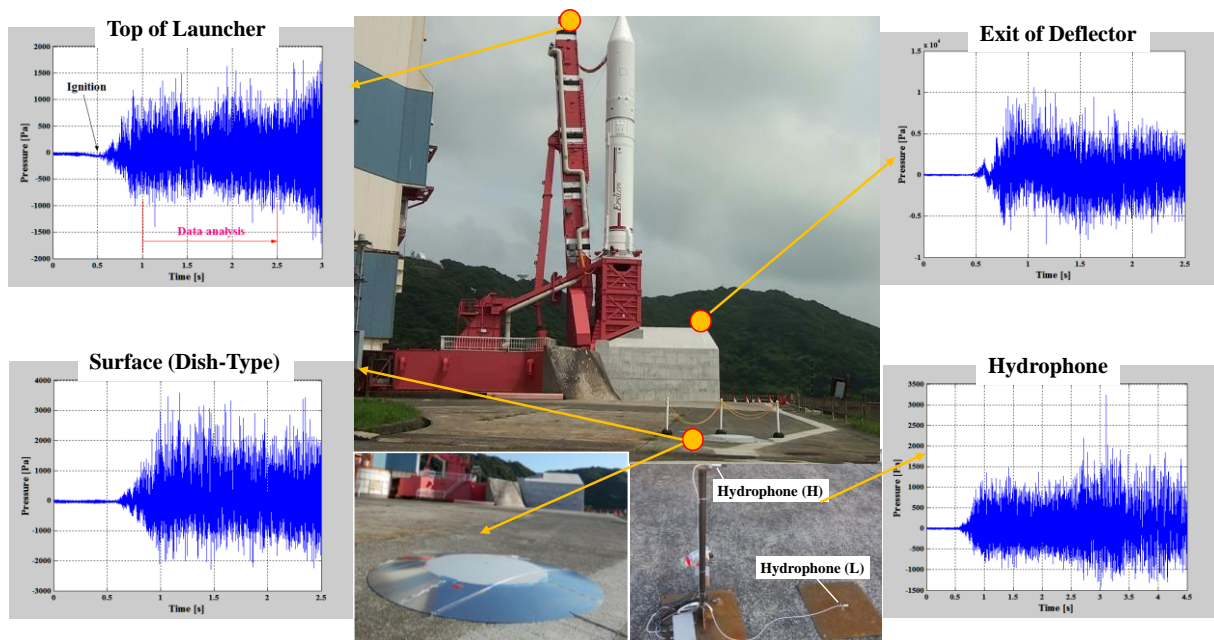

Fig. 16. Time data obtained at representative positions during lift-off of the first Epsilon launch vehicle. Positions are at the top of launcher, at the exit of deflector, on the ground surface (Dish-type), and on a stand (Hydrophone).
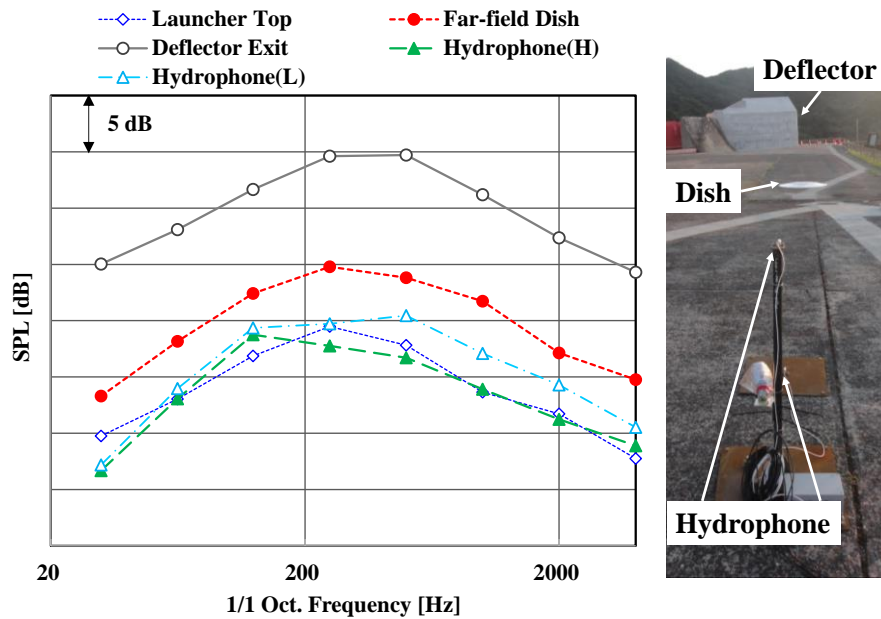
Fig. 17. Octave band levels obtained at the top of the launcher, at the exit of the deflector, on the ground away from the deflector ("dish" ground surface and hydrophones).

5   SUMMARY

A beamforming system consisting of a 9-arm foldable array, a front-end and software including beamforming calculation with shading and diagonal removal, was applied to tests of scale-models of a launch pad. The results were successfully used to compare the sound attenuation of the difference launch pad scale-models.

Secondly, the use of hydrophone was proposed for measuring the rocket launch, showing the ability of hydrophones as an alternative transducer to ordinary microphones for measuring high sound pressure levels in air.

ACKNOWLEDGEMENTS

REFERENCES

[1]   J. Hald and J.J. Christensen, "A novel beamformer design for noise source location from intermediate measurement distances", Proceedings of ASA/IFA/MIA (2002).

[2]   J.J. Christensen and J. Hald, "Beamforming", Brüel & Kjær Technical Review no. 1, pp. 1–48. (2004).

[3]   J. Hald, "Combined NAH and Beamforming Using the Same Array", Brüel & Kjær Technical Review no. 1, pp. 11–39. (2005).

[4]   J. Hald, Y. Ishii, T. Ishii, H. Oinuma, K. Nagai, Y. Yokoyama, and K. Yamamoto. "High-resolution fly-over Beamforming using a small practical array." AIAA 2012-2229, 2012. 18th AIAA/CEAS Aeroacoustics Conference, Colorado Springs, Co, 4-6 June 2012

[5]   Y. Ishii, J. Hald, T. Ishii, H. Oinuma, K. Nagai, Y. Yokoyama, and K. Yamamoto. "High-resolution fly-over beamforming using a practical array." BeBeC-2014-16, 2014. 5th Berlin Beamforming Conference, 19-20 February, 2014.

[6]   S. Gade, J. Hald, B. Ginn, "Noise Source Identification with Increased Spatial Resolution", Sound & Vibration Magazine April 2013, pp 9-13 (2013)

[7]   S. Gade, J. Hald, J. Gomes, G. Dirks and B. Ginn "Recent advances in Road Vehicle Moving Source Beamforming" JSAE paper No. 20145014, (2014)

[8]   http://global.jaxa.jp/projects/rockets/epsilon/

[9]   K. Ui, K. Minesugi, K. Terashima, S. Tsutsumi, T. Ishii, K. Kishi, et al. "Development of Structure, Mechanism and Mechanical Environment of Epsilon Launch Vehicle", Aeronautical and Space Sciences Japan, Vol. 60-1, 8-14, 2012 (in Japanese).

[10] K. Ui, K. Minesugi, K. Goto, T. Kamita, T. Ishii, S. Tsutsumi, and K. Kishi. "The Evaluation of the Structure Subsystem and the Environment Conditions of the First Flight Test of the Epsilon Launch Vehicle." STCP-2013-012, 2014. Proceedings of Space Transportation Symposium FY2013, Kanagawa Japan, 16-17 January 2014(in Japanese).

[11] T. Ishii, S. Tsutsumi, K. Ui, S. Tokudome, and K. Wada. "Acoustic Measurement of Subscale Rocket Boosters." AJCPP2012-083, 2012. Asian Joint Conference on Propulsion and Power, Xi'an, China, 1-4 March 2012.

[12] S. Tsutsumi, T. Ishii, K. Ui, S. Tokudome, K. Wada, "Study on AcousticPrediction and Reduction of Epsilon Launch Vehicle at Liftoff," Journal of Spacecraft and Rockets, 2015, Vol.52, pp.350-361.

[13] Ehrenfried, K. and Koop, L., "A comparison of iterative deconvolution algorithms for the mapping of acoustic sources," AIAA Paper 2006-2711.

[14] T. Ishii, K. Yamamoto, K. Nagai, and Y. Ishii. "Overview of Jet Noise Measurement at JAXA." Trans. JSASS Aerospace Tech., Vol.12, 123-132, 2014.

[15] T. Ishii, S. Tsutsumi, K. Ui, S. Tokudome, Y. Ishii, K. Wada, and S. Nakamura. "Acoustic Measurement of 1:42 Scale Booster and Launch Pad." Proceedings of Meeting on Acoustics POMA 18, 040009, 2014. 164th Meeting of the Acoustical Society of America, Kansas City, MO, 22-26 October 2012.

[16] T. Ishii, S. Tsutsumi, K. Ui, H. Oinuma, Y. Ishii, and K. Wada. "Acoustic measurements of the Epsilon rocket at liftoff." J. Acoust. Soc. Am. 134, 4056, 2013. 166th Meeting of the Acoustical Society of America, San Francisco, CA, 2-6 December 2013.

[17] S. Tsutsumi, T. Ishii, K. Ui, S. Tokudome, and K. Wada. "Assessing Prediction and Reduction Technique of Lift-off Acoustics Using Epsilon Flight Data." AIAA 2015-1007, 2015. 53rd AIAA Aerospace Sciences Meeting, Kissimmee, FL, 5-9 January 2015.